27th EPS Conference on Contr. Fusion and Plasma Phys. Budapest, 12-16 June 2000 ECA Vol. **24B** *(2000) 560 -563*

The Physics of Confinement Improvement with Impurity Seeding in DIII–D

M. Murakami,[1] G.R. McKee,[2] G.L.Jackson,[3] G.M. Staebler,[3] D.R. Baker,[3] J.A. Boedo,[4] N.H. Brooks,[3] K.H. Burrell,[3] D.R. Ernst,[5] T. E. Evans,[3] C.M. Greenfield,[3] R.J. Groebner,[3] J.E. Kinsey,[6] R.J. La Haye,[3] L.L. Lao,[3] A. Messiaen,[7] J. Mandrekas,[8] J. Ongena,[7] C.L. Rettig,[9] B.W. Rice,[10] D.W. Ross,[11] H.E. St John,[3] R.D. Sydora,[12] D.M. Thomas,[3] M.R. Wade,[1] W.P. West,[3] and the DIII–D Team

[1]*Oak Rid ge National Laboratory, Oak Ridge, Tennessee 37381, USA*
[2]*University of Wisconsin, Madison, Wisconsin 53706, USA*
[3]*General Atomics, P.O. Box 85608, San Diego, California 92186-5608, USA*
[4]*University of California, San Diego, California 92093, USA*
[5]*Princeton Plasma Physics laboratory, Princeton, New Jersey 08543*
[6]*Lehigh University, Bethlehem, Pennsylvania 18015*
[7]*KMS/ERM, Brussels, Belgium*
[8]*Georgia Institute of Technology, Atlanta, Georgia 30332, USA*
[9]*University of California, Los Angels, California 90095, USA*
[10]*Lawrence Livermore National Laboratory, Livermore, California 94550, USA*
[11]*University of Texas, Austin, Texas 78712*
[12]*University of Alberta, Edmonton, AB T6G2J1, Canada*

Clear increases in confinement (from $H_{89P}\approx1$ to $H_{89P}\leq2$) and simultaneous reductions of long-wavelength turbulence have been observed in L–mode discharges in DIII–D, which are directly correlated with external impurity injection [1]. These observations provide an opportunity to understand the mechanism for confinement improvement with impurity seeding observed in a number of tokamaks [2], and to make quantitative tests of theory-based turbulence and transport models with experimental measurements. Impurity seeding can be used not only to produce a radiative mantle to reduce heat fluxes to the first wall material [3], but also as a tool to control profiles in Advanced Tokamak (AT) plasmas.

Significant confinement improvements are observed with injection of noble gases (Ne, Ar, and Kr) into L–mode edge, negative central shear (sawtooth-free) discharges in DIII–D. Compared to similar reference discharges without impurity injection, confinement enhancement factor and neutron emission in neon-injected discharges are nearly doubled [Fig. 1(a,b)]. The ion and electron temperature with neon injection exhibit increased central values and profile broadening while the electron density profile becomes more peaked.

Transport analysis shows that reductions of transport coefficients with neon injection are observed in all transport channels. The analysis is carried out using the TRANSP code [4]. Effective charge (Z_{eff}) profiles are determined from charge exchange recombination (CER) measurements of fully ionized carbon and neon density, and the central value increases from 1.5 (reference) to ≤3.4 (full neon). The modest dilution of the main fuel ions is compensated by an increased averaged density and an increased peaking factor, resulting in the deuteron density nearly the same in both discharges. The factor of 2 increase in neutrons results primarily from an increase in thermal neutrons. Ion thermal diffusivity (χ_i) at the normalized radius ρ = 0.65 in the full neon case is quickly (within <50 ms) decreased by factor of 3, followed by a gradual reduction [Fig. 1(d)]. The radial profile of χ_i at the peak performance time (t = 1.65 s) is shown in Fig. 1(f), indicating that χ_i is reduced throughout the profile, approaching neoclassical levels calculated by the NCLASS model [5]. The electron thermal diffusivity (χ_e) shows a modest (≤1.5) reduction throughout the neon injection period [Fig. 1(e)]. Both toroidal momentum and particle diffusivity decrease with neon injection. Therefore all transport channels are improved with neon injection. An impurity species scan (Ne, Ar, and Kr) with a fixed radiative loss fraction ($P_{rad}/P_{in} \approx 0.75$) shows the improvement of confinement and reduction of transport coefficients are largest in these plasmas on DIII–D with lower atomic number for which the impurity charge fraction is the largest.

Observed reductions of both long and short wavelength fluctuations are correlated with reductions of ion and electron thermal transport, respectively. Long-wavelength ($0 < k_\theta <$

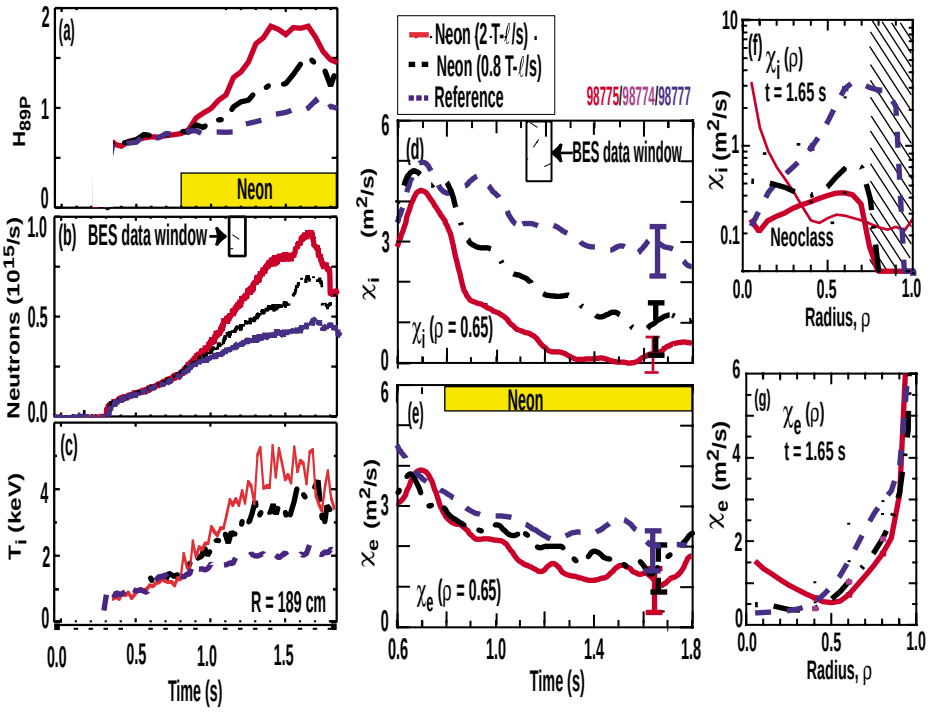

Fig. 1. Characteristics of plasma parameters for discharges with full neon (solid), half neon (chain) and a reference discharge without neon (dashed): (a) energy confinement enhancement factor, (b) neutrons, (c) central ion temperature, (d) evolution of ion and (e) electron thermal diffusivity at $\rho = 0.65$, (f) ion and (g) electron thermal diffusivity profiles at t=1.65 s. The error bars in (d) and (e) represent uncertainty in assigning the convection power. The shaded area for $\rho > 0.8$ in (f) and (g) represents power balance uncertainties.

3 cm^{-1}) density fluctuations measured with Beam Emission Spectroscopy (BES) [Fig. 2] and Far Infrared (FIR) scattering show that long-wavelength turbulence ($k_\theta \rho_s \leq 0.6$ where ρ_s is the ion gyroradius evaluated at the sound speed) turbulence is dramatically reduced in the core (at $\rho \leq 0.7$). Both diagnostics exhibit a fast drop in fluctuation amplitude (within 10–20 ms) right after neon injection followed by a slow reduction. These features are in the $\chi_i(t)$ behavior, but the fast decay of χ_i tends to be is slowed by averaging processes in transport analysis. Reduced edge turbulent particle flux is observed with edge Langmuir probes, which also correlates well with the confinement improvement. Preliminary analysis of short wavelength fluctuations measured with FIR scattering (k_θ = 13 cm^{-1} at $\rho = 0.65 \pm 0.15$) shows that the RMS amplitude decreases in a bursting fashion during impurity injection. The average fluctuation level is correlated well with electron thermal diffusivity as impurity quantities and species are varied. Uncertainties of the source of these fluctuations exists because of the luck of a large E×B Doppler shift in the fluctuation spectrum. The observed (non-suppressed) fluctuations must exist where the E×B drift is small, such as near magnetic axis.

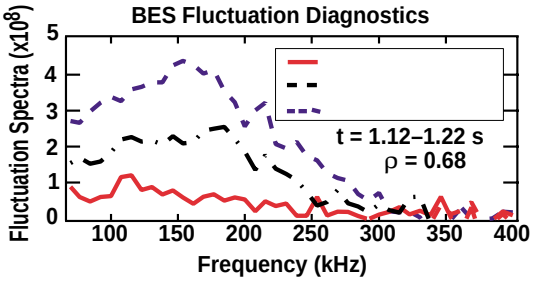

Fig. 2. Effects of varying neon quantity on BES spectra.

A physical mechanism that causes the observed reduction in turbulence and transport is suggested from the effect of impurities on the reduction of growth rate of toroidal drift wave turbulence and the increase in radial electric field shear. The long wavelength turbulence observed is largely driven by ion temperature gradient (ITG) and trapped electron modes (TEM) [6]. Various studies have shown that impurities can affect the stability of these microinstabilities, and have observed that peaked impurity density profiles tend to stabilize ITG modes as a result of one of several mechanisms: dilution of the main ions, direct mode

stabilization by impurity ions, and temperature gradient changes due to enhanced localized radiation. In addition, E×B shearing affects the stabilization of micro-turbulence [7]. In the E×B shearing model, turbulence is suppressed as the shearing rate ($\omega_{E\times B}$) exceeds the linear growth rate of the most unstable modes, $\omega_{E\times B} > \gamma_{max}$ due to eddy shearing and nonlinear decorrelation. Linear growth rates were calculated by the gyrokinetic stability (GKS) code [8] using measured plasma profiles without taking into account the radial electric field. The E×B shearing rates [9] were calculated from radial force balance of the intrinsic carbon ions based on CER measurements of toroidal and poloidal rotation and pressure gradient.

In the discharges with neon injection, the E×B shearing rate significantly exceeds the linear growth rate of turbulence. Figure 3 shows the calculated maximum growth rates and shearing rate as a function of the normalized radius at t=1.16 s. Two changes occur in the neon discharge relative to the reference discharge. At $\rho = 0.65$ which is close to the fluctuation measurement location, the maximum growth rate is reduced by a factor of 1.7, while $\omega_{E\times B}$ is increased by a factor of 2.3, thus achieving the conditions, $\gamma_{max}/\omega_{E\times B} = 1/4 < 1$. It is noted that impurity injection expands the stabilization radius ($\gamma_{max}/\omega_{E\times B} \approx 1$), an important feature for controlling E×B shearing induced ITB in AT operation. Simulations with the FULL code including electric field rotation [10] shows that ITG/TEM growth rate are reduced substantially by neon injection alone, but inclusion of the E_r effect completely stabilizes the modes. Predictions of fully saturated turbulence levels have been calculated by a 3-dimensional gyrokinetic particle simulation code [11], showing a reduced saturated density fluctuation amplitude with neon injection [1]. Nonlinear gyrofluid simulations using GRYFFIN for the reference case has been compared with the BES turbulent spectra and TRANSP-calculated transport fluxes [12]. Simulated k-spectra for the reference case is similar to the BES spectra (with the amplitude overestimated by a factor of ≈3). The resulting simulated ion thermal flux is in agreement with the experiment, implying that the turbulence nearly accounts for the observed ion thermal flux for the reference case.

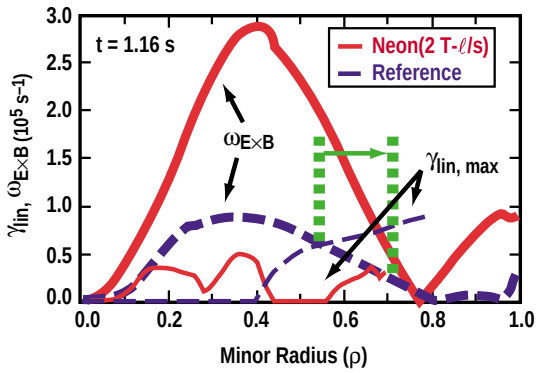

Fig. 3. Comparison of maximum linear growth rates (fine) and E×B shearing rates (bold) in a neon-injected (solid) and reference (dashed) discharge at t = 1.16s.

The E×B shearing rate continues to rise while the maximum growth rate is reduced during neon injection, as shown in Fig. 4 for the two discharges at $\rho = 0.65$. The plasma profiles also evolve, and they do so in a manner which further reduces turbulence. For example, the density profile peaking factor, and the parameter, $\eta_e = L_{ne}/L_{Te}$, important in the electron temperature gradient mode, decreases (Fig. 5). In order to facilitate understanding of relative importance of these effects, the Gyro Landau fluid model, GLF23 [14], is being incorporated into transport codes.

Recent experiments examined the confinement improvement effects of neon injection at higher toroidal field in order to expand the operation space of RI–mode plasmas. We found that neon injected into a discharge at B_T= 2.0 T and I_p = 1.5 MA did not improve confinement as much as the 1.6 T case with the same q_{95}, particularly in the early phase of the neon injection as shown in Fig. 6(a), and the fluctuation reduction with neon injection was smaller [Fig. 6(c)]. This was found to be partially due to lower neon content in the core plasma ($Z_{eff}(0)$ was 2.5 as opposed to 3.4

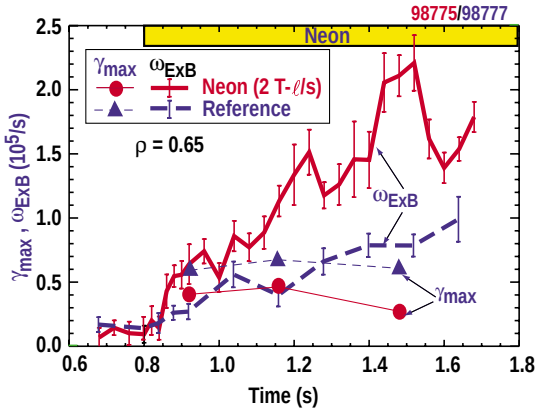

Fig. 4. Time evolution of the E×B shearing rates (curves with error bars) and maximum linear growth rates (curves with solid circles and triangles) in a neon-injected and reference discharge.

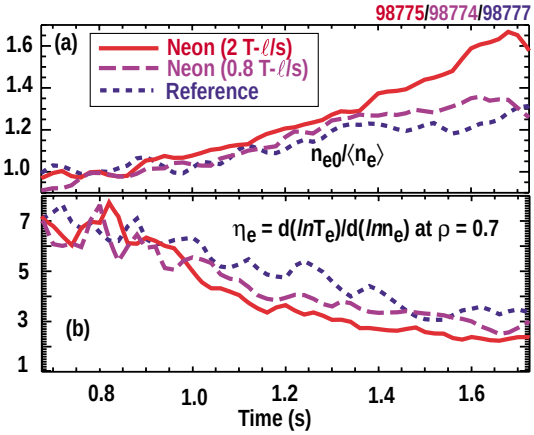

Fig. 5. Time evolution of (a) density peaking factor and (b) η_e (ratio of electron temperature and density gradients.

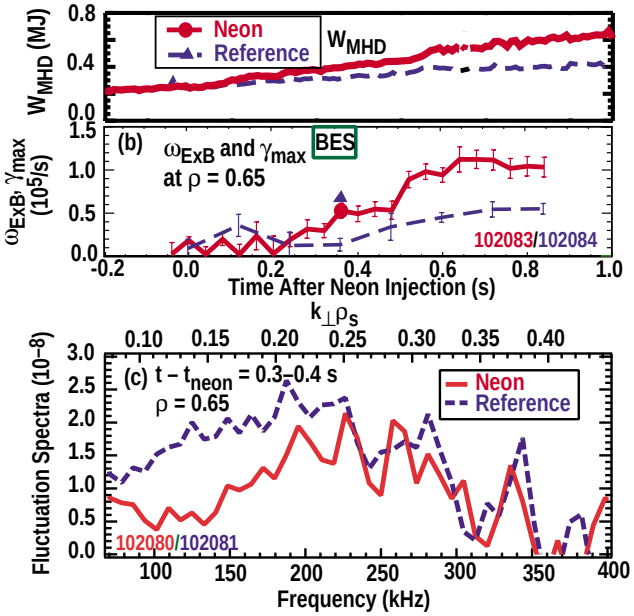

Fig. 6. Evolution of discharge characteristics with (solid) and without (dashed) neon injection at B_T=2.0 T and I_p = 1.6 MA: (a) energy confinement time, (b) E×B shearing rate; and (c) BES fluctuation spectra measured at 0.3–0.4 s after neon injection.

at 1.6 T). This resulted from a smaller neon puff, and more favorable divertor pumping geometry due to the plasma shape used. To pursue further, Fig. 6(b) shows the ω_{ExB} is about a factor of 2 lower than for the 1.6 T case. The maximum growth rate calculated at the time of the BES observation coincides with ω_{ExB} in the neon-injected discharge. The marginal E×B shearing may explain why the observed spectra shows a neon-induced reduction only at longer wavelengths [Fig. 6(c)], because E×B shearing is more effective in reducing long wavelength turbulence. It is noted at 0.6 s after the neon puff, $\omega_{E\times B}$ "spontaneously" increased to a higher value. At the same time the stored energy increased by 20%. The spontaneous transition has been seen in earlier DIII–D experiments with impurity injection in ELMing H-mode plasmas [3]. Subsequent experiments at the same B_T and I_p with a larger neon puff and less favorable neon pumping geometry have produced energy confinement times (τ_E) as good as at 1.6 T. Nevertheless, normalized confinement (e.g., H_{89P}) is considerably lower than at 1.6 T, further indicating there may be an inverse B_T dependence in this confinement improvement mechanism. Further investigations are underway.

In summary, significant confinement improvement is observed with injection of noble gas into L–mode edge discharges. Neon produces the largest confinement improvement, compared with Ar and Kr. Transport reduction is observed in all transport channels during impurity injection, with the most significant being in the ion channel. Long wavelength turbulence reduction is correlated well with the transport reduction. Both gyrokinetic analysis and simulations indicate the transport reductions are due to combined effects of impurity-induced stabilization of microinstabilities and E×B shear suppression. These mechanisms appear to be at work for limiter tokamaks.

[1] G.R. McKee, M. Murakami *et al*., Phys. Plasmas **7**, 1870 (2000).
[2] J. Ongena, *et al*. Plasma Phys. Controlled Fusion **41** A379 (1999), and references therein.
[3] G.L. Jackson, M. Murakami, D.R. Baker *et al*., submitted to Nucl. Fusion (2000).
[4] R.J. Hawryluk et al., *Physics Close to Thermonuclear Conditions*, Varenna, Italy, 1979 (Commission of European Communities, Brussels, 1979).
[5] W.A. Houlberg, , Phys. Plasmas **4**, 3230 (1997).
[6] W. Horton, Rev. Mod. Phys. **71**, 735 (1999) and references therein.
[7] K.H. Burrell, Phys. Plasmas 4, 1499 (1997), and references therein.
[8] R.E. Waltz, R.L. Dewar, and X. Garbet, Phys. Plasmas **5**, 1784 (1998).
[9] T.S. Hahm and K.H. Burrell, Phys. Plasmas 2, 1648 (1995).
[10] G. Rewoldt *et al*., Phys. Plasmas **5**, 1815 (1998).
[11] R.D. Sydora, *et al*., Plasma Phys. Controlled Fusion **38**, A281 (1996).
[12] D.W. Ross *et al*., Report, U. Texas, Austin (2000).
[13] M.J. Tokar, J. Ongena, *et al*., Phys. Rev. Lett., 84, 895 (2000).
[14] R.E. Waltz and R.L. Miller, Phys. Plasmas **6**, 4265 (1999).